

# Squeezed single-atom laser in a photonic crystal

Rong Tan<sup>a</sup>, Gao-xiang Li<sup>a,\*</sup> and Zbigniew Ficek<sup>b</sup>

<sup>a</sup>Department of Physics, Huazhong Normal University, Wuhan 430079, China

<sup>b</sup>Department of Physics, School of Physical Sciences, The University of Queensland, Brisbane, Australia 4072

(Dated: October 26, 2018)

We study non-classical and spectral properties of a strongly driven single-atom laser engineered within a photonic crystal that facilitates a frequency-dependent reservoir. In these studies, we apply a dressed atom model approach to derive the master equation of the system and study the properties of the dressed laser under the frequency dependent transition rates. By going beyond the secular approximation in the dressed-atom cavity-field interaction, we find that if, in addition, the non-secular terms are included into the dynamics of the system, then non-linear processes can occur that lead to interesting new aspects of cavity field behavior. We calculate variances of the quadrature phase amplitudes and the incoherent part of the spectrum of the cavity field and show that they differ qualitatively from those observed under the secular approximation. In particular, it is found that the non-linear processes lead to squeezing of the fluctuations of the cavity field below the quantum shot noise limit. The squeezing depends on the relative population of the dressed states of the system and is found only if there is no population inversion between the dressed states. Furthermore, we find a linewidth narrowing below the quantum limit in the spectrum of the cavity field that is achieved only when the secular approximation is not made. An interpretation of the linewidth narrowing is provided in terms of two phase dependent noise (squeezing) spectra that make up the incoherent spectrum. We establish that the linewidth narrowing is due to squeezing of the fluctuations in one quadrature phase components of the cavity field.

PACS numbers: 42.55.Tv, 42.50.Ct, 42.50.Ar

## I. INTRODUCTION

A single-atom laser, in which no more than one atom is present in an optical resonator, is one of the key systems to study quantum effects in the interaction of electromagnetic fields with matter [1, 2, 3, 4, 5]. Although a single-atom laser is admittedly an elementary model, it has the advantage over a multi-atom laser that in any practical realization of the laser one is not concerned with many difficulties such as fluctuations of the number of atoms. With the present trapping and cooling techniques, the atom can easily be localized in a small region within the Lamb-Dicke regime. Because of its simplicity, many quantum features of single-atom lasers, such as sub-Poissonian photon statistics, photon antibunching, squeezing and vacuum Rabi splitting have been predicted and experimentally observed [6, 7].

The primary obstacle in the realization of one-atom lasers is spontaneous emission. The reason is that spontaneous emission is a source of noise that leads to emission of photons into modes different from the cavity mode. Therefore, it is not surprising that many schemes have been proposed to reduce spontaneous emission. It has been demonstrated that spontaneous emission can be reduced if an atom is located in a squeezed vacuum [8], or inside a cavity that facilitates an exclusive spatial selection of radiation modes coupled to the atom [9, 10, 11, 12]. The cavity appears as a frequency filter for spontaneous emission. A further reduction of spontaneous emission can be achieved through a dynamical means that unlike the conventional method of coupling an atom into the cavity mode, one could first drive the atom with a strong

laser field and then couple the resulting dressed-atom system with the cavity mode [13, 14]. When the Rabi frequency of the driving laser is much larger than the cavity bandwidth, one can tune the cavity mode to one of the dressed-atom transition frequencies thereby eliminating spontaneous emission on the other transitions. Within this approach, a wide variety of quantum and spectral features, such as atomic population inversion [15, 16, 17], and dynamical suppression and narrowing of the spectral lines [18, 19] has been predicted and some of them verified experimentally [20, 21, 22, 23].

Recently, Florescu *et al.* [24] have applied the dressed-atom approach to a single-atom laser that incorporates the dynamical suppression of spontaneous emission inside a photonic crystal. They have applied the secular approximation in the coupling of a dressed two-level atom to the cavity mode that the Rabi frequency of the dressing field is much larger than the coupling constant between the atom and the cavity field. By appropriate tuning of the cavity mode and the dressed-atom transition frequencies, they have shown that the variances of the cavity field amplitude and the linewidth of the cavity field spectrum can be reduced to the quantum shot noise limit. These effects result from the filtering property of the photonic crystal that effectively forms a frequency dependent reservoir of a specific spectral function (step function) of the radiation modes. A photonic crystal that is a periodic dielectric structure, can prohibit light propagation over a continuous range of frequencies, irrespective of the direction of propagation [25, 26]. It is also known that in photonic crystals extremely small micro-cavity mode volumes and very high cavity  $Q$  factors can be realized [27, 28, 29]. It is associated with the unique properties of photonic crystals, i.e., the photonic density of states within or near a photonic band gap can almost vanish or exhibit discontinuous changes as a function of frequency with appropriate engineering, which is essentially different from its free-space counterpart.

---

\*Electronic address: gaox@phy.cnu.edu.cn

Although the secular approximation is often entirely adequate to describe the interaction of the cavity field with a dressed-atom system, there are circumstances when the non-secular terms might be important, for example in the strong coupling limit of the cavity field to the dressed-atom system. One could argue that even under these circumstances, the non-secular terms would only make small corrections to the dynamics of the system. In the following, we show that this is not the case, they may lead to new aspects of cavity field behavior that differ qualitatively from those observed under the secular approximation. To show this, the dressed-atom approach for a driven two-level atom placed inside a photonic crystal is generalized to deal with non-secular terms in the atom-cavity field interaction. The method used in this paper is similar to that used by Florescu *et al.* [24] but with one significant difference, we do not make the secular approximation in the coupling of the cavity mode to the dressed-atom system. Instead, we consider the role of the non-secular terms in the operation of a strongly driven single-atom laser. We present solutions for the steady-state variance of the quadrature components of the cavity field amplitude and the incoherent part of the spectrum of the cavity field. In the course of the calculations, we observe that the inclusion of the non-secular terms results in a *double* coupling of the cavity field to the dressed atom and leads to non-linear terms in the master equation of the system that reflect a possibility of non-linear processes between the dressed states when the secular approximation is not made. Our results demonstrate that these non-linear processes lead to the reduction of the fluctuations of the cavity field amplitude below the quantum shot noise limit. In addition, we find that the spectral line of the cavity field may now be narrowed below the quantum limit giving a subnatural linewidth of the emitted field. A qualitative understanding of the origin of the line narrowing is obtained by writing the incoherent part of the cavity field spectrum in terms of the phase dependent noise (squeezing) spectra. We show that the narrowing results from negative values of the squeezing spectrum of one quadrature phase component of the field.

The paper is organized as follows. In Sec. II, we present the model Hamiltonian and derive the master equation for a strongly driven two-level atom coupled to a single-mode cavity and placed inside a photonic band gap material that acts as a frequency dependent reservoir. In Sec. III, we derive the basic equations of motion for the expectation values of the atomic and field correlation functions and find their steady-state values. We then apply them in Sec. IV to investigate variances of the quadrature phase components of the cavity field that determine the fluctuations of the cavity field amplitude, and in Sec. V to the calculations of the spectrum of the cavity field. We calculate the incoherent part of the spectrum and then analyze its properties in terms of the squeezing spectra. Finally, we summarize the results in Sec. VI.

## II. MASTER EQUATION

We consider a single two-level atom with ground state  $|1\rangle$  and excited state  $|2\rangle$  separated by the transition frequency  $\omega_a$ .

The atom is coupled to a single mode of a high- $Q$  microcavity engineered within a photonic crystal with coupling constant  $g$ , and is driven by a coherent external laser field of a frequency  $\omega_L$  and the resonant Rabi frequency  $\epsilon$ . In addition, the atom is damped at the rate  $\gamma$  by spontaneous emission to modes other than the cavity mode. In practice this model can be realized by embedding a quantum dot in a dielectric microcavity (defect) placed within a two-mode waveguide channel in a 2D PBG microchip [24]. In a photonic band gap material, one mode of the waveguide channel is engineered to produce a large discontinuity in the local photon density of states near the atom, and another mode is used to propagate the pump beam. By suitable engineering, it is possible to realize a strong coupling of the quantum dot to both the pumping waveguide mode and the high- $Q$  cavity mode [24]. For simplicity, we treat the driving external field classically and work in the interaction picture. The total system is described by a Hamiltonian that under the electric-dipole and the rotating-wave approximations can be written as

$$H = H_0 + H_1, \quad (1)$$

where the first term

$$H_0 = \hbar\Delta_c a^\dagger a + \frac{1}{2}\hbar\Delta_a \sigma_3 + \hbar\epsilon(\sigma_{12} + \sigma_{21}) + \hbar \sum_{\lambda} \Delta_{\lambda} a_{\lambda}^{\dagger} a_{\lambda} \quad (2)$$

is the noninteracting Hamiltonian of the driven atom plus the cavity mode plus the photonic crystal radiation reservoir modes, and the second term

$$H_1 = i\hbar g(a^\dagger \sigma_{12} - \sigma_{21} a) + i\hbar \sum_{\lambda} g_{\lambda}(\omega_{\lambda})(a_{\lambda}^{\dagger} \sigma_{12} - \sigma_{21} a_{\lambda}) \quad (3)$$

is the interaction Hamiltonian between the atom and the cavity mode and the photonic crystal vacuum radiation modes.

Here,  $a$  and  $a^\dagger$  are the cavity-mode annihilation and creation operators,  $a_{\lambda}$  and  $a_{\lambda}^\dagger$  are the photonic crystal radiation reservoir annihilation and creation operators,  $\sigma_{ij}$  are the bare atomic operators,  $\sigma_{ij} = |i\rangle\langle j|$  ( $i, j = 1, 2$ ), and  $\sigma_3 = \sigma_{22} - \sigma_{11}$  describes the bare atomic inversion. The parameter  $\Delta_a = \omega_a - \omega_L$  denotes the detuning of the atomic resonance frequency  $\omega_a$  from the frequency  $\omega_L$  of the driving laser field,  $\Delta_c = \omega_c - \omega_L$  is the detuning of the cavity frequency from the frequency of the laser field, and  $\Delta_{\lambda} = \omega_{\lambda} - \omega_L$  is the detuning of the reservoir frequency  $\omega_{\lambda}$  of a mode  $\lambda$  from the laser frequency.

The coefficient  $g$  describes the strength of the coupling between the atom and the cavity mode that we assume to be constant independent of frequency, and  $g_{\lambda}(\omega_{\lambda})$  describes the strength of the coupling between the atom and the vacuum modes of the photonic crystal. It contains the information about the frequency dependent mode structure of the photonic crystal and can be written as

$$g_{\lambda}(\omega_{\lambda}) = g_{\lambda} D(\omega_{\lambda}), \quad (4)$$

where  $g_\lambda$  is a constant proportional to the dipole moment of the atom, and  $D(\omega_\lambda)$  is the transfer function of the photonic crystal, the absolute value square of which can be identified as the Airy function of a frequency dependent radiation reservoir [30].

The explicit form of  $D(\omega_\lambda)$  depends on the type of radiation reservoir used. For a photonic band gap material, the transfer function is in the form of the unit step function  $|D(\omega_\lambda)|^2 = u(\omega_\lambda - \omega_b)$ , where  $\omega_b$  is the photonic density of states band edge frequency. Thus,  $|D(\omega_\lambda)|^2 = 0$  for  $\omega_\lambda < \omega_b$  and  $|D(\omega_\lambda)|^2 = 1$  for  $\omega_\lambda > \omega_b$ . Since the frequencies  $\omega_\lambda < \omega_b$  are forbidden in the band gap material, it is possible to selectively eliminate spontaneous emission at some frequencies of the driven atom.

The strong driving field can be viewed as a dressing field for the atom. Therefore, we begin by diagonalizing the atomic part of the Hamiltonian together with the interaction of the atom with the laser field

$$H_{af} = \frac{1}{2}\hbar\Delta_a\sigma_3 + \hbar\epsilon(\sigma_{12} + \sigma_{21}), \quad (5)$$

to find the eigenstates (dressed states) of the combined atom plus driving field system. Since the driving field is treated classically in our calculations, we find the so-called semiclassical dressed states

$$\begin{aligned} |\tilde{1}\rangle &= \cos\phi|1\rangle + \sin\phi|2\rangle, \\ |\tilde{2}\rangle &= \sin\phi|1\rangle - \cos\phi|2\rangle, \end{aligned} \quad (6)$$

where  $\cos^2\phi = (1 + \Delta_a/\Omega)/2$  with the angle  $\phi$  defined such that  $0 \leq \phi \leq \pi/2$ . The dressed states form non-degenerate doublets that are separated in energy by  $\hbar\omega_L$ , and the states of the doublet are split by  $\hbar 2\Omega$ , where  $\Omega = (4\epsilon^2 + \Delta_a^2)^{1/2}$  is the Rabi frequency of the detuned field.

We now couple the dressed states to the cavity field and to the photonic crystal vacuum modes. First, we replace the atomic operators by the dressed-state operators

$$\begin{aligned} \sigma_{12} &= -\frac{1}{2}\sin(2\phi)R_3 + \sin^2\phi R_{21} - \cos^2\phi R_{12}, \\ \sigma_{21} &= -\frac{1}{2}\sin(2\phi)R_3 + \sin^2\phi R_{12} - \cos^2\phi R_{21}, \\ \sigma_3 &= -\cos(2\phi)R_3 + \sin(2\phi)(R_{12} + R_{21}), \end{aligned} \quad (7)$$

where  $R_{ij} = |\tilde{i}\rangle\langle\tilde{j}|$  are the dressed-atom dipole operators and  $R_3 = R_{22} - R_{11}$ . Next, we perform the unitary "dressing" transformation of the interaction Hamiltonian

$$\tilde{H}_1 = \exp(i\tilde{H}_0 t)H_1 \exp(-i\tilde{H}_0 t), \quad (8)$$

with

$$\tilde{H}_0 = \Omega R_3 + \Delta_c a^\dagger a + \sum_\lambda \Delta_\lambda a_\lambda^\dagger a_\lambda, \quad (9)$$

and obtain the interaction Hamiltonian between the dressed atom and both the cavity mode and the photonic crystal vac-

uum modes

$$\begin{aligned} \tilde{H}_1 &= i\hbar g \left( sca^\dagger R_3 e^{i\Delta_c t} + c^2 a^\dagger R_{12} e^{i(\Delta_c - 2\Omega)t} \right. \\ &\quad \left. - s^2 a^\dagger R_{21} e^{i(\Delta_c + 2\Omega)t} - \text{H.c.} \right) \\ &+ i\hbar \sum_\lambda g_\lambda \left( sca_\lambda^\dagger R_3 e^{i\Delta_\lambda t} + c^2 a_\lambda^\dagger R_{12} e^{i(\Delta_\lambda - 2\Omega)t} \right. \\ &\quad \left. - s^2 a_\lambda^\dagger R_{21} e^{i(\Delta_\lambda + 2\Omega)t} - \text{H.c.} \right), \end{aligned} \quad (10)$$

where  $s = \sin\phi$  and  $c = \cos\phi$ .

The Hamiltonian (10) describes the interaction of the dressed atom with the cavity field and with the vacuum modes. We see that in the dressed-atom picture, the cavity frequency and the vacuum modes are tuned to the dressed-state transitions that occur at three characteristic frequencies,  $\Delta_c$  and  $\Delta_c \pm 2\Omega$ . By matching the cavity field frequency to one of the dressed states frequencies, we may manipulate the strength of the interaction between the driven system and the cavity mode.

Our aim is to derive from the Hamiltonian (10) the master equation for a reduced density operator of the driven atom and the cavity field. It is obtained by tracing the density operator of the total system over the photonic crystal radiation reservoir variables. On carrying out this procedure, it is found that in the dissipative part of the master equation certain terms are slowly varying in time while the others are oscillating with frequencies  $2\Omega$  and  $4\Omega$ . Since we are interested in the case where the Rabi frequency  $\Omega$  is much larger than the atomic and cavity damping rates

$$\Omega \gg \gamma, \kappa, \quad (11)$$

we can invoke the secular approximation that consists of dropping these rapidly oscillating terms. These terms, if kept in the master equation, would make corrections to the dynamics of the system of the order of  $\gamma/\Omega$ , and thus completely negligible. We therefore find that after discarding the rapidly oscillating terms in the dissipative part of the master equation, the time evolution of the reduced density operator is of the form

$$\begin{aligned} \frac{\partial \rho}{\partial t} &= gsc[a^\dagger R_3 e^{i\Delta_c t} - a R_3 e^{-i\Delta_c t}, \rho] \\ &+ gc^2[a^\dagger R_{12} e^{i(\Delta_c - 2\Omega)t} - a R_{21} e^{-i(\Delta_c - 2\Omega)t}, \rho] \\ &- gs^2[a^\dagger R_{21} e^{i(\Delta_c + 2\Omega)t} - a R_{12} e^{-i(\Delta_c + 2\Omega)t}, \rho] \\ &+ \mathcal{L}_a \rho + \mathcal{L}_c \rho, \end{aligned} \quad (12)$$

where

$$\begin{aligned} \mathcal{L}_a \rho &= \frac{1}{2}\gamma_0 (R_3 \rho R_3 - \rho) + \frac{1}{2}\gamma_- (R_{21} \rho R_{12} - R_{12} R_{21} \rho) \\ &+ \frac{1}{2}\gamma_+ (R_{12} \rho R_{21} - R_{21} R_{12} \rho) + \text{H.c.} \\ \mathcal{L}_c \rho &= \frac{1}{2}\kappa (2a\rho a^\dagger - a^\dagger a \rho - \rho a^\dagger a), \end{aligned}$$

describe spontaneous dynamics between the dressed states of the system and of the cavity mode, respectively. The param-

ters

$$\begin{aligned}\gamma_0 &= s^2 c^2 \gamma |D(\omega_L)|^2 + (c^2 - s^2) \gamma_p, \\ \gamma_- &= s^4 \gamma |D(\omega_L - 2\Omega)|^2 + 4s^2 c^2 \gamma_p, \\ \gamma_+ &= c^4 \gamma |D(\omega_L + 2\Omega)|^2 + 4s^2 c^2 \gamma_p\end{aligned}\quad (13)$$

determine the damping rates between the dressed states of the system. They also include the contribution of the dephasing rate  $\gamma_p$  which may arise from scattering of phonons of the host crystal on the atom embedded in the solid part of the dielectric material. The coefficient  $\gamma_0$  corresponds to spontaneous emission occurring at two transitions of the dressed atom; One from the lower dressed state  $|\tilde{1}\rangle$  to the lower dressed state of the manifold below and the other from the upper dressed state  $|\tilde{2}\rangle$  to the upper dressed state of the manifold below. These transitions occur at frequency  $\omega_L$ . The coefficient  $\gamma_+$  corresponds to spontaneous emission from the upper dressed state to the lower dressed state of the manifold below and occurs at frequency  $\omega_L + 2\Omega$ , whereas the coefficient  $\gamma_-$  corresponds to spontaneous emission from the lower dressed state to the upper dressed state of the manifold below and occurs at frequency  $\omega_L - 2\Omega$ .

An essential feature of the master equation (12) is the presence of the oscillatory terms in the coherent part of the evolution involving the dressed atom and the cavity field. In experimental practice it might imply that there is no restriction on the relation between the Rabi frequency  $\Omega$  and the coupling constant  $g$ , and the master equation can be applied to both situations, where the coupling constant  $g$  is much smaller or comparable to the Rabi frequency.

As we have already mentioned, we work in the strong-coupling regime of  $\Omega \gg g \gg \gamma, \kappa$ . The latter inequality has been invoked into Eq. (12) to neglect the effect of non-secular terms in the dissipative part of the master equation, but to keep the non-secular terms in the interaction of the cavity field with the dressed atom. This condition is satisfied in a typical band-gap material, where strong couplings  $g$  and significant reductions of the spontaneous emission rate  $\gamma$  are easily achieved due to the confinement of the atom to an extremely small volume with a significantly suppressed density of the vacuum modes. For example, given the electric dipole moment of an atom of  $\mu \approx 10^{-29} \text{ C m}^{-1}$  and the cavity mode volume of  $V \approx 10^{-6} \text{ m}^3$ , then the atom cavity coupling will be  $g \approx 10^{10} \text{ Hz}$  [24, 27]. With the spontaneous emission rate of the atom in a free space of  $\gamma \approx 10^8 \text{ Hz}$ , the inequality  $g \gg \gamma$  is easily satisfied. The parameter  $\kappa$ , that describes the damping of the cavity field, is equal to zero in an ideal cavity. However, in a realistic structure  $\kappa \neq 0$ , that arises from a weak coupling of the cavity mode to the waveguide mode of the band-gap material. This coupling may result from defects or disorders in the waveguide channel caused by the manufacturing process that can be kept at a minimal level [24, 26, 27, 29]. Effectively, the waveguide channel acts as an external reservoir of vacuum modes to which photons can escape from the cavity mode. Thus, the inequality  $g \gg \gamma, \kappa$  is realistic and should be easy to satisfy within the current band-gap material technology.

In the following, we focus on the case of  $\Delta_c \approx 0$ , i.e., the

cavity field tuned close to the central frequency of the dressed atom. In this limit, the master equation (12) contains terms that are time independent and thus corresponding to the resonant interaction of the cavity field with the dressed atom. It also contains terms that have an explicit time dependence of the form  $\exp(\pm 2i\Omega t)$ . These terms correspond to a dispersive (non-resonant) interaction of the cavity field with the dressed atom, which induces interesting new property as we will show below.

We first perform a canonical transformation of the master equation (12) by

$$\tilde{\rho} = \exp(i\Delta_c a^\dagger a t) \rho \exp(-i\Delta_c a^\dagger a t), \quad (14)$$

and find that the master equation for the transformed density operator takes the form

$$\frac{\partial \tilde{\rho}}{\partial t} = -i [H'_0 + H'(t), \tilde{\rho}] + \mathcal{L}_a \tilde{\rho} + \mathcal{L}_c \tilde{\rho}, \quad (15)$$

where

$$\begin{aligned}H'_0 &= gsc (a^\dagger R_3 - a R_3) + \Delta_c a^\dagger a, \\ H'(t) &= ig [(c^2 a^\dagger + s^2 a) R_{12} e^{-i2\Omega t} - \text{H.c.}].\end{aligned}\quad (16)$$

Note that the Hamiltonian  $H'(t)$  disappears under the secular approximation on the interaction of the dressed-atom with the cavity field. Due to the presence of the rapidly oscillating terms, the Hamiltonian  $H'(t)$  can be treated as a perturber to the time-independent Hamiltonian  $H'_0$ . Since  $g \ll \Omega$ , we can perform a second-order perturbation calculations with respect to  $g$  and find an effective Hamiltonian [31] that can be written as

$$\begin{aligned}H'_{\text{eff}} &= -iH'(t) \int H'(t') dt' = \frac{\hbar g^2}{2\Omega} [s^2 c^2 R_3 (a^2 + a^{\dagger 2}) \\ &\quad + (s^4 + c^4) \left( R_3 a^\dagger a + \frac{1}{2} R_3 \right)].\end{aligned}\quad (17)$$

In this case, the master equation (12) takes the form

$$\begin{aligned}\frac{\partial \tilde{\rho}}{\partial t} &= -i \left[ \left( \Delta_c + \frac{g_2^2}{2\Omega} R_3 \right) a^\dagger a, \tilde{\rho} \right] - i \frac{g_2^2}{4\Omega} [R_3, \tilde{\rho}] \\ &\quad + g_1 [(a^\dagger - a) R_3, \tilde{\rho}] - i \frac{g_1^2}{2\Omega} [R_3 (a^2 + a^{\dagger 2}), \tilde{\rho}] \\ &\quad + \mathcal{L}_a \tilde{\rho} + \mathcal{L}_c \tilde{\rho},\end{aligned}\quad (18)$$

where

$$g_1 = gsc \quad \text{and} \quad g_2 = g\sqrt{(s^4 + c^4)} \quad (19)$$

are the "effective" coupling constants of the cavity field to the dressed-atom system.

The important new feature of the master equation (18) is in the presence of an additional non-linear terms that results in an effective *double* coupling of the cavity field to the dressed atom. The first term on the right-hand side of Eq. (18) represents a shift of the cavity frequency. It includes a dressed-atom inversion dependent shift that arises solely from the non-secular terms in the dressed-atom picture. The second term

represents a shift of the dressed-atom frequencies that also arises from the presence of the non-secular terms. The third term represents a resonant coupling of the cavity field to the dressed atom at frequency  $\omega_c \approx \omega_L$ , and finally the fourth term describes a dispersive coupling through the off-resonant Rabi sideband frequencies and is determined by non-linear two-photon absorption and emission processes between the dressed states. Thus, the presence of the non-secular terms results in the non-linear coupling of the cavity field to the dressed atom and shifts of the cavity and dressed-atom resonance frequencies. The amplitude of these contributions is of order  $g^2/\Omega$  and therefore is small, but not necessarily too small to make detectable contributions to the dynamics of the system. In what follows, we shall show that the non-linear terms in the master equation (18) play in fact an important role in the dynamics of the system and will study in details non-classical and spectral properties of the out-put field of the laser operating with a resonator engineered in a photonic band gap material.

### III. EQUATIONS OF MOTION

In this section we investigate the influence of the non-secular terms on the properties of a driven single-atom laser. The properties can all be expressed in terms of single-time and two-time expectation values of the dressed-atom and the cavity field operators. The master equation (18) enables us to derive equations of motion for expectation values of an arbitrary combination of the atomic and cavity field operators. In particular, for the dressed-atom population inversion and the cavity field amplitudes, we find the following closed set of equations of motions

$$\begin{aligned} \frac{d}{dt}\langle R_3 \rangle &= -\gamma_2 - \gamma_1 \langle R_3 \rangle, \\ \frac{d}{dt}\langle a \rangle &= -\left(\frac{1}{2}\kappa - i\Delta_c\right)\langle a \rangle + g_1 \langle R_3 \rangle \\ &\quad - i\frac{g_2^2}{2\Omega}\langle R_3 a \rangle - i\frac{g_1^2}{\Omega}\langle R_3 a^\dagger \rangle, \\ \frac{d}{dt}\langle R_3 a \rangle &= g_1 - \left(\gamma_1 + \frac{1}{2}\kappa - i\Delta_c\right)\langle R_3 a \rangle \\ &\quad - \gamma_2 \langle a \rangle - i\frac{g_2^2}{2\Omega}\langle a \rangle - i\frac{g_1^2}{\Omega}\langle a^\dagger \rangle, \end{aligned} \quad (20)$$

and equations of motion for  $\langle a^\dagger \rangle$  and  $\langle R_3 a^\dagger \rangle$  are obtained by Hermitian conjugate of the above equations.

For the expectation values involving higher order combinations of the operators, such as the number of photons, the mas-

ter equation leads to the following set of equations of motion

$$\begin{aligned} \frac{d}{dt}\langle a^\dagger a \rangle &= -\kappa \langle a^\dagger a \rangle + g_1 (\langle R_3 a^\dagger \rangle + \langle R_3 a \rangle) \\ &\quad - i\frac{g_1^2}{\Omega} (\langle R_3 a^{\dagger 2} \rangle - \langle R_3 a^2 \rangle), \\ \frac{d}{dt}\langle a^{\dagger 2} \rangle &= i\frac{g_1^2}{\Omega}\langle R_3 \rangle - (\kappa + 2i\Delta_c)\langle a^{\dagger 2} \rangle + 2g_1 \langle R_3 a^\dagger \rangle \\ &\quad + i\frac{g_2^2}{\Omega}\langle R_3 a^{\dagger 2} \rangle + 2i\frac{g_1^2}{\Omega}\langle R_3 a^\dagger a \rangle, \\ \frac{d}{dt}\langle R_3 a^{\dagger 2} \rangle &= i\frac{g_1^2}{\Omega} - (\gamma_1 + \kappa + 2i\Delta_c)\langle R_3 a^{\dagger 2} \rangle + 2g_1 \langle a^\dagger \rangle \\ &\quad - \gamma_2 \langle a^{\dagger 2} \rangle + i\frac{g_2^2}{\Omega}\langle a^{\dagger 2} \rangle + 2i\frac{g_1^2}{\Omega}\langle a^\dagger a \rangle, \\ \frac{d}{dt}\langle R_3 a^\dagger a \rangle &= -(\gamma_1 + \kappa)\langle R_3 a^\dagger a \rangle + g_1 (\langle a^\dagger \rangle + \langle a \rangle) \\ &\quad - \gamma_2 \langle a^\dagger a \rangle - i\frac{g_1^2}{\Omega} (\langle a^{\dagger 2} \rangle - \langle a^2 \rangle), \end{aligned} \quad (21)$$

and equations of motion for  $\langle a^2 \rangle$  and  $\langle R_3 a^2 \rangle$  are obtained by the Hermitian conjugate of the equations of motion for  $\langle a^{\dagger 2} \rangle$  and  $\langle R_3 a^{\dagger 2} \rangle$ , respectively.

The quantities  $\gamma_1$  and  $\gamma_2$  occurring in Eqs (20) and (21) are given in terms of the damping rates  $\gamma_+$  and  $\gamma_-$ , and are defined as

$$\begin{aligned} \gamma_1 &= \gamma_+ c^4 + \gamma_- s^4 + 8\gamma_p s^2 c^2, \\ \gamma_2 &= \gamma_+ c^4 - \gamma_- s^4. \end{aligned} \quad (22)$$

We see that the quantities  $\gamma_1$  and  $\gamma_2$  depend only on the transition rates centered at the dressed states resonances corresponding to the Rabi sidebands. Moreover, the quantity  $\gamma_2$  can be negative, whereas  $\gamma_1$  is positive for all values of the parameters involved. In addition,  $\gamma_1 \geq \gamma_2$  even in the absence of the dephasing process,  $\gamma_p = 0$ .

### IV. STEADY-STATE SOLUTIONS

We proceed here to discuss the steady-state properties of the correlation functions for  $\Delta_c = 0$  that are listed in Appendix I. In this simplified case, we obtain solutions in a physically transparent form that will allow one to gain physical insight into how the non-secular terms and structured band gap material can modify the properties of the dressed-atom system and the cavity field. The exact steady-state solutions of Eqs. (20) and (21), valid for an arbitrary detuning  $\Delta_c$  are quite lengthy and will be computed numerically in the next section.

Before commencing our analysis of the properties of the cavity field, we first look into properties of the dressed atom. We observe that the equation of motion for the expectation value of the atomic operator  $R_3$  is decoupled from the remaining equations. Hence, it has a simple steady-state solution

$$\langle R_3 \rangle = -\frac{\gamma_2}{\gamma_1}. \quad (23)$$

This shows that the steady-state value of the dressed inversion operator is not affected by the non-secular terms. However,

it depends crucially on the quantities  $\gamma_1$  and  $\gamma_2$  that, on the other hand, depend on the mode structure of the band gap material. The inversion varies between  $+1$  and  $-1$  corresponding to locking the population in the dressed state  $|\bar{2}\rangle$  and  $|\bar{1}\rangle$ , respectively. According to Eq. (22), it happens when there is no spontaneous emission on one of the Rabi frequency of the dressed system.

Let us now examine the stationary properties of the cavity field. In the steady-state regime and for the case of the cavity frequency and the atomic transition frequency tuned on resonance with the central frequency of the dressed-atom system,  $\Delta_c = 0$  and  $\Delta_a = 0$ , the expectation values of the cavity field operators can be expressed as

$$\begin{aligned} \langle a \rangle &= -\frac{2g_1\gamma_2}{\gamma_1\kappa} \left[ 1 + i\frac{4g_1^2\gamma_1}{\kappa\gamma_2\Omega} - i\frac{8g_1^2(\gamma_1^2 - \gamma_2^2)}{\kappa\gamma_2(2\gamma_1 + \kappa)\Omega} \right], \\ \langle a^2 \rangle &= \frac{4g_1^2}{\kappa^2} \left[ 1 - \frac{2(\gamma_1^2 - \gamma_2^2)}{\gamma_1(2\gamma_1 + \kappa)} \right] \\ &\quad + i\frac{g_1^2\gamma_2}{\kappa\gamma_1\Omega} \left\{ 1 + \frac{32g_1^2}{\kappa^2} \left[ 1 - \frac{(3\kappa + 4\gamma_1)(\gamma_1^2 - \gamma_2^2)}{(\kappa + \gamma_1)(\kappa + 2\gamma_1)^2} \right] \right\} \\ &\quad - \frac{2g_1^4}{\kappa^2\Omega^2} \left\{ 1 - \frac{(\gamma_1^2 - \gamma_2^2)}{\gamma_1(\gamma_1 + \kappa)} \right. \\ &\quad \left. + \frac{32g_1^2}{\kappa^2} \left[ 1 - \frac{u(\gamma_1^2 - \gamma_2^2)}{\gamma_1(\gamma_1 + \kappa)^2(2\gamma_1 + \kappa)^2} \right] \right\}, \\ \langle a^\dagger a \rangle &= \frac{4g_1^2}{\kappa^2} \left( 1 - \frac{2(\gamma_1^2 - \gamma_2^2)}{\gamma_1(2\gamma_1 + \kappa)} + \frac{g_1^2}{2\Omega^2} \left\{ 1 - \frac{(\gamma_1^2 - \gamma_2^2)}{\gamma_1(\gamma_1 + \kappa)} \right. \right. \\ &\quad \left. \left. + \frac{32g_1^2}{\kappa^2} \left[ 1 - \frac{u(\gamma_1^2 - \gamma_2^2)}{\gamma_1(\gamma_1 + \kappa)^2(2\gamma_1 + \kappa)^2} \right] \right\} \right), \quad (25) \end{aligned}$$

where  $u = (\gamma_1 + \kappa)(2\gamma_1 + \kappa)(2\gamma_1 + 3\kappa) + (4\gamma_1 + 3\kappa)\gamma_2^2$ . Similarly to the dressed-atom inversion, the properties of the expectation values of the cavity field depend on the parameters  $\gamma_1$  and  $\gamma_2$  and thus are also sensitive to the mode structure of the band gap material. A particular situation of interest is that of  $\gamma_1 = \gamma_2$  which, according to Eq. (22) occurs when the dephasing rate  $\gamma_p = 0$  and the lower Rabi sideband frequency is adjusted to be inside the forbidden frequency region of the band gap material,  $\gamma_- = 0$ . As we see from Eq. (25), the cavity field correlation functions are then enhanced due to the combined effect of the band gap material and the non-secular processes.

The non-secular terms not only enhance the number of photons, but also lead to a shift of the cavity resonance frequency. This is shown in Fig. 1, where we plot the steady-state expectation value of the number of photons in the cavity field as a function of the detuning  $\Delta_c$  in the band gap material configuration  $\gamma_- = 0$ , in which spontaneous emission is forbidden at the lower Rabi sideband frequency. The graphs are computed from the exact steady-state solution of Eq. (21) that is presented in the Appendix I. It is evident that in the presence of the non-secular terms the number of photons attains the maximum value in the vicinity of the detuning  $\Delta_c = -0.16\gamma$ . The shift of the maximum towards the negative detuning  $\Delta_c$  indi-

cates a pulling of the oscillation frequency of the cavity field away from the passive cavity frequency  $\omega_c$  towards the lower Rabi sideband frequency that is inside the forbidden frequency region of the band gap material. This is another noteworthy feature of the non-secular terms in the dressed-atom picture.

We note here that the values of the parameters used to plot Fig. 1 are consistent with the good cavity limit assumed in the derivation of the master equation (18) and are experimentally realistic. We have discussed the validity of the good cavity limit in Sec. II for realistic parameters of our system, and have shown that a small cavity damping and a large atom cavity coupling  $g$  can be readily achieved within the current band-gap material technology [24, 27].

## V. FLUCTUATIONS OF THE CAVITY FIELD

We now proceed to investigate the fluctuations of the cavity field amplitude by analyzing the variances of the conjugate quadrature phase amplitudes  $X_+ = ae^{i\theta} + a^\dagger e^{-i\theta}$  and  $X_- = -i(ae^{i\theta} - a^\dagger e^{-i\theta})$ , where  $\theta$  is the quadrature phase. Previous calculations of Florescu *et al.* [24] have shown that under the secular approximation and by appropriate tuning of the dressed-atom transition frequencies to the band gap material mode transfer structure, the fluctuations of the cavity field can be reduced down up to the quantum shot noise limit. We now consider the possibility of using the non-secular processes to reduce the quantum fluctuations below the quantum limit. There is a good reason to believe that the non-secular processes can modify the fluctuations of the cavity field am-

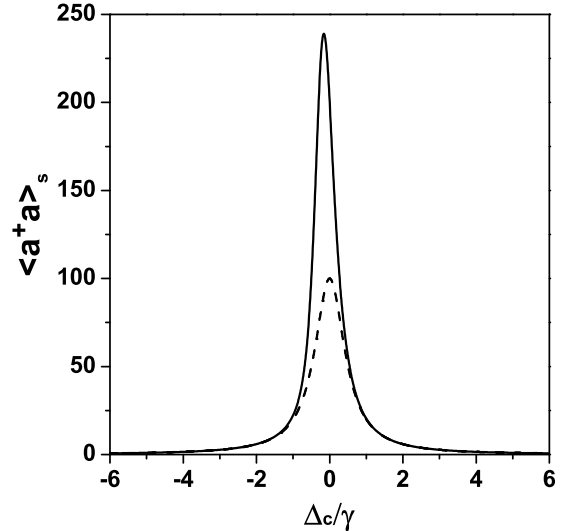


FIG. 1: The steady-state expectation value of the number of photons in the cavity field plotted as a function of the detuning  $\Delta_c$  in the presence (solid line) and in the absence (dashed line) of the non-secular terms for  $\Omega = 100\gamma$ ,  $\gamma_+ = 10\gamma$ ,  $\kappa = 0.1\gamma_+$ ,  $g = 10\kappa$ ,  $\Delta_a = 0$ , and  $\gamma_- = \gamma_p = 0$ .

plitude. They appear as non-linear processes and it is well known that these processes are typical sources used to generate squeezed light [8].

Let us first examine the normally ordered variance of the quadrature component  $X_+$  for the simplified case of  $\Delta_c = 0$ . This analysis provides simple analytical formulas for the variance and illustrates the role of the non-secular processes in the behavior of the cavity field. To determine the variance, we make use Eq. (25) and find that it can be expressed as

$$\langle : (\Delta X_+)^2 : \rangle_s = S_1 + S_2, \quad (26)$$

where

$$S_1 = \frac{8g_1^2(\gamma_1^2 - \gamma_2^2)}{\kappa\gamma_1^2(\kappa + 2\gamma_1)}(1 + \cos 2\theta) \quad (27)$$

is the contribution of the linear interaction term, and

$$S_2 = -\frac{2g_1^2\gamma_2 \sin 2\theta}{\kappa\gamma_1\Omega} \left[ 1 + \frac{32g_1^2(\gamma_1^2 - \gamma_2^2)(3\gamma_1 + 2\kappa)}{\kappa\gamma_1(\kappa + \gamma_1)(\kappa + 2\gamma_1)^2} \right] + \frac{4g_1^4(1 - \cos 2\theta)}{\kappa^2\Omega^2} \left\{ 1 - \frac{(\gamma_1^2 - \gamma_2^2)}{\gamma_1(\kappa + \gamma_1)} \right. \quad (28)$$

$$\left. + \frac{32g_1^2(\gamma_1^2 - \gamma_2^2) [\kappa\gamma_1(\kappa + \gamma_1) + (5\gamma_1 + 4\kappa)\gamma_2^2]}{\kappa\gamma_1^2(\kappa + \gamma_1)^2(\kappa + 2\gamma_1)^2} \right\}$$

is the contribution from the non-secular terms.

Clearly,  $S_1 \geq 0$  and  $S_2$  vanishes under the secular approximation. Note that the term  $S_2$  is negative for the phase angle  $0 < \theta < \pi/2$  and  $\gamma_2$  positive. Thus, for an appropriate choice of the parameters, the fluctuations of the cavity field can be squeezed below the quantum shot noise level. However, when we examine Eqs. (27) and (28), we find that the  $S_1$  term exceeds the  $S_2$  term independent of the values of the parameters involved. This means that squeezing is possible only when the term  $S_1$  is suppressed. Inspection of Eq. (28) shows that the  $S_1$  term is suppressed when  $\gamma_1 = \gamma_2$ . According to Eq. (22), this conditions can be achieved by suppressing spontaneous emission on transitions at the lower Rabi frequency  $\omega_L - 2\Omega$ . Thus, the immediate consequence of the fact that  $\gamma_1 = \gamma_2$  is that the dominating positive term  $S_1$  vanishes, leaving the variance depending solely on the term  $S_2$  that arises from the presence of the non-linear processes between the dressed states. Note the dependence of the "squeezer", the  $S_2$  term of the variance, on the ratio  $\gamma_2/\gamma_1$  that according to Eq. (23) determines the inversion between the dressed states. Apparently, for phase angles  $0 < \theta < \pi/2$ , squeezing is obtained only when  $\gamma_2 > 0$ , i.e. when there is no inversion between the dressed states and vice versa, for phase angles  $\pi/2 < \theta < \pi$ , squeezing is obtained for a negative  $\gamma_2$ , i.e. when there is an inversion between the dressed states. Moreover, the optimal condition for squeezing is to maintain  $\gamma_1 = \gamma_2$ . These analysis indicate that a photonic band gap material can be employed to generate a squeezed field from a single-atom laser.

Figure 2 shows the normally ordered variance  $\langle : (\Delta X_+)^2 : \rangle_s$  as a function of the quadrature phase angle  $\theta$ . As the phase change, the variance oscillates from negative to positive values. Negative values mean squeezing of the fluctuations of

the quadrature phase amplitude below the quantum shot noise level. The maximum negative value of the variance, corresponding to the maximum squeezing occurs at  $\theta \approx 0.55$ . However, the maximum value of squeezing obtained for  $\Delta_c = 0$  might not be the greatest value possible due to the shift of the cavity resonance. Actually, it appears for a detuning slightly shifted from the cavity resonance. This is shown in Fig. 3, where we plot the variance as a function of the scaled Rabi frequency  $\epsilon/\Delta_a$ , for  $\gamma_1 = \gamma_2$  and different detunings  $\Delta_c$ . We see that the variance is negative for all values of the Rabi frequency, thus indicating that the cavity field can be in a squeezed state irrespective of the strength of the laser field. As the Rabi frequency increases, the variance decreases and then saturates to a constant value. The saturation level decreases with increasing negative detuning  $\Delta_c$  and attains the maximal negative value, corresponding to the maximum squeezing, for  $\Delta_c = -0.26\gamma$ .

We may conclude this section that the filtering properties of the band gap material and the treatment of the interaction between the cavity field and the dressed atom beyond the secular approximation produces important modifications in the variance of the quadrature field amplitudes, greatly reducing the fluctuations below the quantum limit.

## VI. SPECTRUM OF THE CAVITY FIELD

In this section we investigate the spectrum of the cavity field and point out one more difference between the secular and non-secular single-atom lasers. It has been shown by Florescu

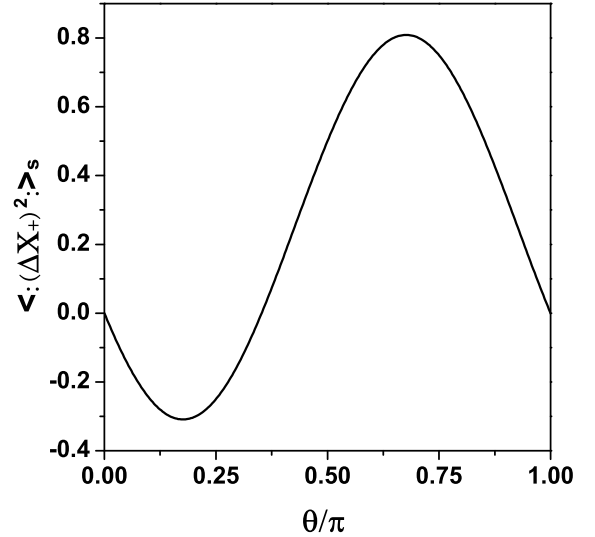


FIG. 2: The steady-state variance  $\langle : (\Delta X_+)^2 : \rangle_s$  of the quadrature component of the cavity field as functions of the quadrature phase  $\theta/\pi$  in a full photonic band gap and for vanishing detuning  $\Delta_c = 0$ . All other parameters are same as in Fig. 1.

*et al.* [24] that in the secular approximation, the spectral line of the cavity field can be narrowed to the quantum limit. Here, we will illustrate that the linewidth of the spectrum can be further reduced that it may go below the quantum limit if the non-secular processes are included into the dynamics of the system.

The steady-state spectrum of the cavity field is defined as the Fourier transform of the two-time correlation function  $\langle a^\dagger(t)a \rangle_s$  of the cavity field operators. In the interaction picture, the spectrum takes the form

$$S(\omega) = 2\text{Re} \int_0^\infty dt e^{i(\omega - \omega_L)t} \langle a^\dagger(t)a \rangle_s, \quad (29)$$

where  $\omega$  is the spectral frequency, the subscript  $s$  represents the average over the steady-state values of the field operators, and the operators without time argument refer to their steady-state values.

We may write the cavity field operators in the form  $a(t) = \langle a(t) \rangle + \delta a(t)$ , where  $\delta a(t)$  are the fluctuations operators that describe fluctuations of the cavity field about its average value. In this case, the spectrum can be decomposed into a sum of two terms

$$S(\omega) = S_{el}(\omega) + S_{in}(\omega), \quad (30)$$

where

$$S_{el}(\omega) = 2\pi \langle a^\dagger \rangle_s \langle a \rangle_s \delta(\omega - \omega_L) \quad (31)$$

is the elastic component of the spectrum, and

$$S_{in}(\omega) = 2\text{Re} \int_0^\infty dt e^{i(\omega - \omega_L)t} \langle a^\dagger(t), a \rangle_s \quad (32)$$

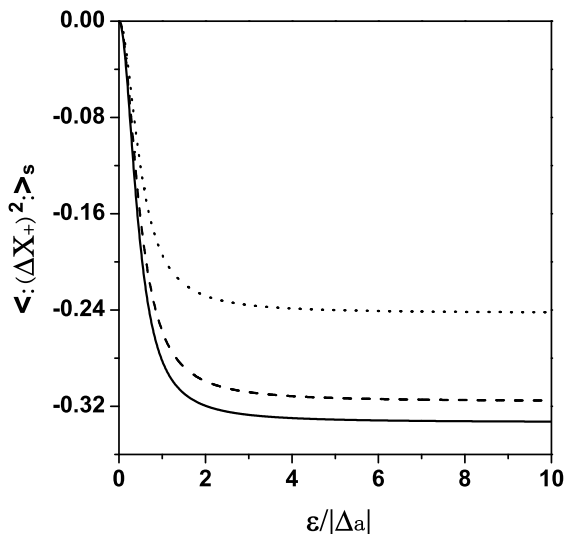


FIG. 3: The normally ordered variance  $\langle : (\Delta X_+)^2 : \rangle_s$  as a function of the scaled Rabi frequency  $\varepsilon / \Delta_a$  in the band gap material configuration of  $\gamma_- = 0$  for  $\theta = 0.8$ ,  $\Omega = 100\gamma$ ,  $\gamma_+ = 10\gamma$ ,  $\kappa = 0.1\gamma_+$ ,  $g = 10\kappa$ ,  $\gamma_p = 0$  and different detunings  $\Delta_c$ :  $\Delta_c = 0$  (dotted line),  $\Delta_c = -0.16\gamma$  (dashed line) and  $\Delta_c = -0.26\gamma$  (solid line).

is the inelastic component with

$$\langle a^\dagger(t), a \rangle_s = \langle a^\dagger(t)a \rangle_s - \langle a^\dagger(t) \rangle_s \langle a \rangle_s. \quad (33)$$

In order to calculate the two-time correlation function appearing in Eq. (32), we make use of the quantum regression theorem [32, 33] from which it is well known that the two-time correlation functions obey the same equations of motion for  $t > 0$  as the corresponding one-time correlation functions. Therefore, we may use Eqs. (20) and (21) to compute the spectrum. The spectrum depends, of course, on the state of the system which we take to be the stationary state.

We will compute numerically the spectra using the equations of motion (20) and (21). However, in order to gain insight into the physics involved, we will present an analytical solution for the case of  $\Delta_c = 0$ .

For purposes of numerical computation, it is convenient to take the Laplace transform of the equations of motion for the correlation functions that transforms them into a set of algebraic equations, and evaluate the spectrum from

$$S_{in}(\omega) = 2\text{Re}[\langle a^\dagger(p), a \rangle_s]_{p=i(\omega - \omega_L)}, \quad (34)$$

where  $p$  is a complex Laplace transform parameter. The exact solution for the Laplace transform of the correlation function with  $\Delta_c = 0$  is given in the Appendix II. We use this exact solution to evaluate the spectrum in the presence of the non-secular processes. We compare the spectra with those obtained under the secular approximation where the non-secular processes are ignored. The results are shown in Figs. 4 and 5.

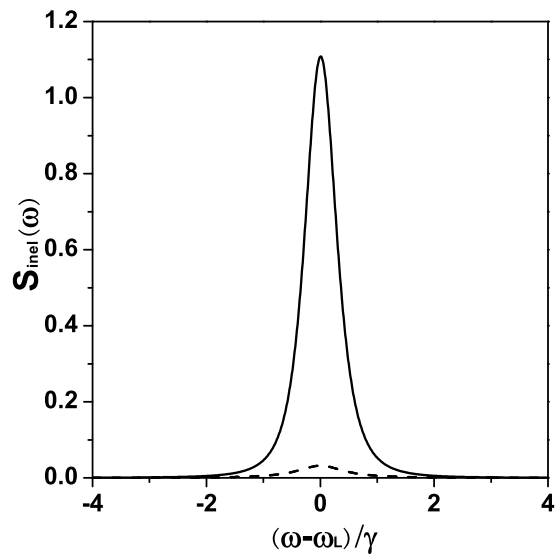


FIG. 4: The incoherent part of the spectrum of the cavity field as a function of the frequency  $(\omega - \omega_L) / \gamma$  calculated with (solid line) and without (dashed line) the non-secular terms for  $\gamma_- / \gamma_+ = 0.0001$  and  $\Delta_c = 0$ . All other parameters are same as in Fig. 1.

Let us first compare the spectra obtained with the non-secular processes with that obtained under the secular approximation. Figure 4 shows the incoherent part of the spectrum of



the cavity field in the band gap material configuration with  $\gamma_- = 0.0001\gamma_+$ . The spectrum consists of a single line centered at frequency  $\omega = \omega_L$  whose the profile depends on whether the non-secular processes are or are not included. The shape of the line is not exactly a Lorentzian when the non-secular processes are included, but becomes a Lorentzian when these processes are ignored. One may notice a significant linewidth narrowing below the natural width when the non-secular processes are included.

Figure 5 illustrates the effect of the cavity detuning on the spectrum. We see that the maximum narrowing of the spectral line actually occurs not at  $\Delta_c = 0$  but for the detuning  $\Delta_c = -0.26\gamma$  that, according to Fig. 3, corresponds to the maximum squeezing in one of the quadrature phase components of the cavity field. This indicates that the spectrum may be directly affected by squeezing in the cavity field.

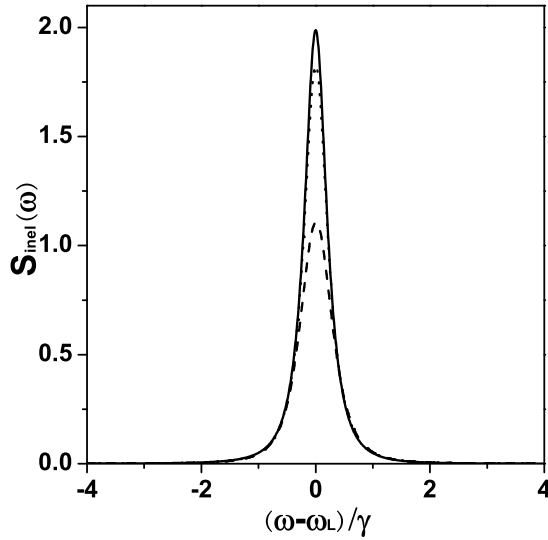


FIG. 5: The incoherent part of the spectrum of the cavity field as a function of the frequency  $(\omega - \omega_L)/\gamma$  for different detunings  $\Delta_c$ :  $\Delta_c = 0$  (dashed line),  $\Delta_c = -0.16$  (dotted line) and  $\Delta_c = -0.26$  (solid line). All other parameters are same as in Fig. 1.

In order to gain insight into the source of the narrowing of the spectral line, we take the limit of  $\Delta_c = \Delta_a = 0$ ,  $\gamma_- = 0$  and derive from the general solution, Eq. (39), a simple analytical formula for the spectrum

$$S_{in}(\omega) = \frac{16\kappa g_1^4}{\Omega^2 [\kappa^2 + 4(\omega - \omega_L)^2]^2}. \quad (35)$$

This result is in marked contrast to that obtained under the secular approximation [24]. In the case of vanishing mode density on the lower Mollow sideband ( $\gamma_- = 0$ , which corresponds to a full photonic band gap) and no dipolar dephasing ( $\gamma_p = 0$ ), the spectrum of the cavity field consists only of the elastic component under the secular approximation [24]. When the non-secular processes are included, the incoherent

part of the spectrum is present and shows an interesting property that instead of being a simple Lorentzian, it is instead in the form of a squared Lorentzian.

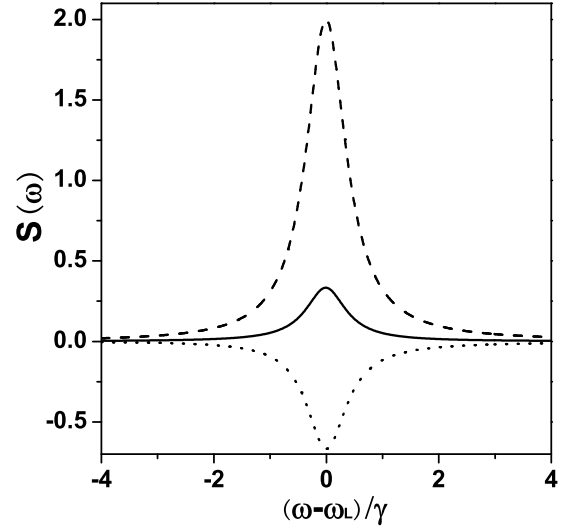


FIG. 6: The incoherent part (solid line) of the cavity field spectrum together with the squeezing spectra  $X_+(\omega)$  (dotted line) and  $X_-(\omega)$  (dashed line) plotted as a function of  $(\omega - \omega_L)/\gamma$  for  $\Delta_c = -0.26\gamma$  and  $\theta = 0.8$ . All other parameters are same as in Fig. 5.

It is well known that a squared Lorentzian can be decomposed into a difference between two Lorentzians [34, 35, 36]. The immediate consequence of one of the Lorentzians being negative is to produce a spectrum which fell off as  $\omega^{-4}$  in the wings, rather than the  $\omega^{-2}$ , which would result if both Lorentzians were positive. It has been shown that the negative weight of one of the Lorentzians can be related to squeezing in the field. Thus, the narrowing of the spectral line, seen in Figs. 4 and 5 can be related to squeezing produced in the non-linear interaction of the cavity field with the dressed atom. Physically, this effect can be best understood and explained in terms of the so-called squeezing spectrum. The incoherent spectrum can be decomposed into the sum of two phase dependent squeezing spectra

$$S_{in}(\omega) = \frac{1}{4} [X_+(\omega) + X_-(\omega)], \quad (36)$$

where

$$\begin{aligned} X_+(\omega) &= \int_{-\infty}^{\infty} dt e^{i(\omega - \omega_L)t} \langle : X_+(t), X_+ : \rangle, \\ X_-(\omega) &= \int_{-\infty}^{\infty} dt e^{i(\omega - \omega_L)t} \langle : X_-(t), X_- : \rangle, \end{aligned} \quad (37)$$

are the squeezing spectra of the normally ordered quadrature phase components of the cavity field amplitude. Negative values in the squeezing spectra indicate squeezed fluctuations of the cavity field.

Figure 6 shows the incoherent spectrum together with the squeezing spectra calculated for the same parameters as in Fig. 5, but with  $\Delta_c = -0.26\gamma$  corresponding to the maximum squeezing in the  $X_+$  quadrature components of the cavity field. We see that the squeezing spectrum  $X_+(\omega)$  is negative over the whole range of frequencies. The fact that  $X_+(\omega)$  is negative indicates that the  $X_+$  quadrature component, that is obtained by an integration of the squeezing spectrum  $X_+(\omega)$  over the frequency  $\omega$ , is squeezed. Thus, we may conclude that the spectral linewidth narrowing is due to the common effect of squeezing and the frequency dependent reservoir formed by the photonic band gap material.

## VII. CONCLUSIONS

We have examined nonclassical and spectral features of a single-atom laser without the use of the secular approximation for the interaction of the cavity field with a dressed-atom system located inside a photonic band gap material. The material appears as a frequency dependent reservoir for the dressed

atom. The inclusion of the non-secular terms leads to an effective double coupling of the cavity field to the dressed states of the system. We have found that by a suitable matching of the dressed-atom transition frequencies to the guiding frequency of the band gap material, it is possible to account for squeezing and narrowing of the spectral line of the cavity field below the quantum shot noise limit. These features are achieved by a combination of a strongly frequency-dependent reservoir and the non-secular processes. The non-linear processes are absent under the secular approximation and present a newly encountered features of a single-atom laser.

## VIII. ACKNOWLEDGMENTS

The authors acknowledge financial support from the National Natural Science Foundation of China (Grant No. 10674052), the Ministry of Education under project NCET (grant no NCET-06-0671) and the National Basic Research Project of China (grant no 2005 CB724508). ZF would like to thank the Huazhong Normal University for hospitality.

- 
- [1] J. Zakrzewski, M. Lewenstein, and T. W. Mossberg, Phys. Rev. A **44**, 7717 (1991).
  - [2] M. Lewenstein, Y. Zhu, and T. W. Mossberg, Phys. Rev. Lett. **64**, 3131 (1990).
  - [3] M. Löffler, G. M. Meyer, and H. Walther, Phys. Rev. A **55**, 3923 (1997).
  - [4] P. Lougovski, F. Casagrande, A. Lulli, and E. Solano, Phys. Rev. A **76**, 033802 (2007).
  - [5] H.-J. Kim, A. H. Khosa, H.-W. Lee, and M. S. Zubairy, Phys. Rev. A **77**, 023817 (2008).
  - [6] J. McKeever, A. Boca, A. D. Boozer, J. R. Buck, and H. J. Kimble, Nature (London) **425**, 268 (2003).
  - [7] T. Pellizzari and H. Ritsch, Phys. Rev. Lett. **72**, 3973 (1994).
  - [8] See e.g. *Quantum Squeezing*, edited by P. D. Drummond and Z. Ficek (Springer-Verlag, Berlin, 2004).
  - [9] E. M. Purcell, Phys. Rev. **69**, 681 (1946).
  - [10] D. Kleppner, Phys. Rev. Lett. **47**, 232 (1981).
  - [11] P. Goy, J. M. Raimond, M. Gross, and S. Haroche, Phys. Rev. Lett. **50**, 1903 (1983).
  - [12] D. J. Heinzen, J. J. Childs, J. E. Thomas, and M. S. Feld, Phys. Rev. Lett. **58**, 1320 (1987).
  - [13] M. Lewenstein, T. W. Mossberg, and R. J. Glauber, Phys. Rev. Lett. **59**, 775 (1987).
  - [14] M. Lewenstein and T. W. Mossberg, Phys. Rev. A **37**, 2048 (1988).
  - [15] C. M. Savage, Phys. Rev. Lett. **60**, 1829 (1988); M. Lindberg and C. M. Savage, Phys. Rev. A **38**, 5182 (1988).
  - [16] T. Quang and H. Freedhoff, Phys. Rev. A **47**, 2285 (1993).
  - [17] P. Zhou and S. Swain, Phys. Rev. A **58**, 1515 (1998); J. S. Peng, G. X. Li, P. Zhou, and S. Swain, Phys. Rev. A **61**, 063807 (2000).
  - [18] H. Freedhoff and T. Quang, Phys. Rev. Lett. **72**, 474 (1994).
  - [19] L. M. Narducci, M. O. Scully, G. L. Oppo, P. Ru, and J. R. Tredicce, Phys. Rev. A **42**, 1630 (1990).
  - [20] Y. Zhu, A. Lezama, and T. W. Mossberg, Phys. Rev. Lett. **61**, 1946 (1988).
  - [21] A. Lezama, Y. Zhu, S. Morin, and T. W. Mossberg, Phys. Rev. A **39**, R2754 (1989).
  - [22] D. J. Gauthier, Y. Zhu, and T. W. Mossberg, Phys. Rev. Lett. **66**, 2460 (1991).
  - [23] W. Lange and H. Walther, Phys. Rev. A **48**, 4551 (1993).
  - [24] L. Florescu, S. John, T. Quang, and R. Z. Wang, Phys. Rev. A **69**, 013816 (2004); L. Florescu, Phys. Rev. A **74**, 063828 (2006).
  - [25] E. Yablonovitch, Phys. Rev. Lett. **58**, 2059 (1987).
  - [26] S. John, Phys. Rev. Lett. **58**, 2486 (1987); S. John and J. Wang, Phys. Rev. Lett. **64**, 2418 (1990); S. John and T. Quang, Phys. Rev. A **50**, 1764 (1994); S. John and T. Quang, Phys. Rev. Lett. **78**, 1888 (1997); S. John and M. Florescu, J. Opt. A, Pure Appl. Opt. **3**, S103 (2001).
  - [27] A. D. Greentree, J. Saltzman, S. Prawer, and L. C. L. Hollenberg, Phys. Rev. A **73**, 013818 (2006).
  - [28] O. Painter, R. K. Lee, A. Scherer, A. Yariv, J. D. O'Brien, P. D. Dapkus, and I. Kim, Science **284**, 1819 (1999).
  - [29] S. John, Phys. Rev. Lett. **53**, 2169 (1984); S. John, Phys. Rev. Lett. **58**, 2486 (1987).
  - [30] A. Yariv, *Quantum Electronics*, 3rd ed. (Wiley, New York, 1989).
  - [31] D. F. V. James, Fortschr. Phys. **48**, 823 (2000).
  - [32] M. Lax, Phys. Rev. **172**, 350 (1968).
  - [33] H. J. Carmichael, *Statistical Methods in Quantum Optics I*, (Springer-Verlag, Berlin, 1999).
  - [34] P. R. Rice and H. J. Carmichael, J. Opt. Soc. Am. B **5**, 1661 (1988).
  - [35] Z. Ficek and S. Swain, J. Opt. Soc. Am. B **14**, 258 (1997); Z. Ficek and J. Seke, Physica A **258**, 477 (1998).
  - [36] J. E. Reiner, W. P. Smith, L. A. Orozco, H. J. Carmichael, and P. R. Rice, J. Opt. Soc. Am. B **18**, 1911 (2001).

## APPENDIX I

In this appendix, we present the exact steady-state solution of the equations of motion (20) and (21) for the case of  $\Delta_c = 0$  that includes all non-secular terms up to the order  $g^4/\Omega^2$ .

$$\langle a \rangle_s = -2g_1[2\alpha F_1 + \gamma_2\kappa(2\gamma_1 + \kappa)^2]/K_1, \quad (38.2)$$

$$\begin{aligned} \langle a^2 \rangle_s &= \{-2(\alpha - \alpha')F_2 + 8g_1^2\alpha F_3\}F_4 \\ &+ 4g_1^2(1 - \frac{4\alpha}{\gamma_2})F_5\}/K_2 - (\alpha - \alpha')/(2\gamma_2), \end{aligned} \quad (38.3)$$

$$\begin{aligned} \langle a^\dagger a \rangle &= 2[(\alpha - \alpha')^2 F_2 - 4g_1^2\alpha(\alpha - \alpha')F_3 \\ &+ 2g_1^2 F_5]/K_2, \end{aligned} \quad (38.4)$$

$$\begin{aligned} \langle R_3 a^\dagger a \rangle_s &= \frac{1}{(\kappa + \gamma_1)K_2\gamma_2}[-2(\alpha - \alpha')^2 x_0 F_2 \\ &+ 8g_1^2\alpha(\alpha - \alpha')x_0 F_3 - 4g_1^2(\gamma_2^2 + 4\alpha(\alpha - \alpha'))F_5 \\ &- 4g_1^2\kappa\gamma_2^2((\kappa + 2\gamma_1)^2 - 4\alpha\alpha')K_3 \\ &- (\alpha - \alpha')^2 K_2/2], \end{aligned} \quad (38.5)$$

$$\begin{aligned} \langle R_3 a \rangle_s &= \frac{2g_1}{K_1}[-4(\kappa\gamma_1 + 2\gamma_2\alpha)\alpha\alpha' \\ &+ 2\gamma_2(\kappa^2 + 4\gamma_2^2 + 4\kappa\gamma_1)\alpha \\ &+ \kappa(\kappa\gamma_1 + 2\gamma_2^2)(2\gamma_1 + \kappa)], \end{aligned} \quad (38.6)$$

$$\begin{aligned} \langle R_3 a^2 \rangle_s &= \frac{2}{(\kappa + \gamma_1)}\{[(\alpha - \alpha')x_1 F_2 - 4g_1^2\alpha x_1 F_3 \\ &+ 2g_1^2 x_2 F_5]/K_2 + x_3/4\}, \end{aligned} \quad (38.7)$$

where

$$\begin{aligned} F_1 &= -4\alpha\alpha'\gamma_1 - 2\gamma_2\kappa\alpha' + (2\gamma_1 + \kappa)(\kappa\gamma_1 + 2\gamma_2^2), \\ F_2 &= 16(\alpha\alpha')^3\gamma_1 \\ &- 4[3\gamma_1(\kappa + \gamma_1)^2 + 2\gamma_1^3 + (\gamma_2^2 - \gamma_1^2)(\kappa + 5\gamma_1)](\alpha\alpha')^2 \\ &+ \{\gamma_1\kappa^2(2\gamma_1 + \kappa)^2 + 2(\kappa + \gamma_1)(\kappa\gamma_1 + \gamma_2^2)[(\kappa + \gamma_1)^2 \\ &+ 2\gamma_2^2 - \gamma_1^2]\}\alpha\alpha' \\ &- \kappa^2(\kappa + \gamma_1)(\kappa\gamma_1 + \gamma_2^2)(2\gamma_1 + \kappa)^2/4, \\ F_3 &= 32(\alpha\alpha')^2\gamma_1 \\ &- 8[(\kappa\gamma_1 + 2\gamma_2^2)(2\gamma_1 + \kappa) + (\kappa + \gamma_1)(\kappa\gamma_1 + \gamma_2^2)]\alpha\alpha' \\ &+ (2\gamma_1 + \kappa)(\gamma_1\kappa + 2\gamma_2^2)(2\kappa^2 + 2\kappa\gamma_1 + \gamma_2^2) \\ &+ \gamma_2^2(2\gamma_1 + \kappa)^2(\gamma_1 + 2\kappa) - 4\gamma_2^2(\gamma_1 + \kappa)(\gamma_1^2 - \gamma_2^2), \\ F_4 &= [\kappa(\kappa + \gamma_1) - 4\alpha\alpha']/\gamma_2 + \alpha + \alpha', \\ F_5 &= -64(\alpha\alpha')^3\gamma_1 \\ &+ 16[(3\kappa\gamma_1 + 2\gamma_2^2)(\kappa + \gamma_1) + \gamma_1(3\gamma_2^2 + \kappa\gamma_1)](\alpha\alpha')^2 \\ &- 4[(\kappa\gamma_1 + 2\gamma_2^2)(2\gamma_1 + \kappa)(2\kappa\gamma_1 + 2\kappa^2 + \gamma_2^2) \\ &+ \gamma_1\kappa^2(\kappa + \gamma_1)^2]\alpha\alpha' \\ &+ \kappa^2(2\gamma_1 + \kappa)(\kappa\gamma_1 + 2\gamma_2^2)(\kappa + \gamma_1)^2, \end{aligned}$$

and

$$\begin{aligned} K_1 &= \{[4\alpha\alpha' - \kappa(2\gamma_1 + \kappa)]^2 - 16\gamma_2^2\alpha\alpha'\}\gamma_1, \\ K_2 &= \{256(\alpha\alpha')^4 - 64(4\kappa^2 + 6\kappa\gamma_1 + 5\gamma_2^2)(\alpha\alpha')^3 \\ &+ 16[2(\kappa^2 + 2\kappa\gamma_1 + 2\gamma_2^2)(2\kappa^2 + 2\kappa\gamma_1 + \gamma_2^2) \\ &+ \kappa^2((2\gamma_1 + \kappa)^2 + (\kappa + \gamma_1)^2)](\alpha\alpha')^2 \\ &- 4\kappa^2[2(\kappa^2 + 2\kappa\gamma_1 + 2\gamma_2^2)(\gamma_1 + \kappa)^2 \\ &+ (2\kappa^2 + 2\kappa\gamma_1 + \gamma_2^2)(\kappa + 2\gamma_1)^2]\alpha\alpha' \\ &+ \kappa^4(\kappa + \gamma_1)^2(\kappa + 2\gamma_1)^2\}\gamma_1, \\ K_3 &= [4\alpha\alpha' - \kappa(\gamma_1 + \kappa)]^2 - 4\gamma_2^2\alpha\alpha', \end{aligned}$$

with

$$\begin{aligned} x_0 &= \gamma_2^2 + \kappa(\kappa + \gamma_1) - 4\alpha\alpha', \\ x_1 &= x_0(\alpha + \alpha')/\gamma_2 + \kappa(\kappa + \gamma_1), \\ x_2 &= -\gamma_2 + 4\alpha(\alpha + \alpha')/\gamma_2, \\ x_3 &= (\alpha^2 - \alpha'^2)/\gamma_2 \\ &- 8g_1^2\kappa\gamma_2[(\kappa + 2\gamma_1)^2 - 4\alpha\alpha']K_3/K_2, \\ \alpha &= i\frac{g^2}{2\Omega}, \\ \alpha' &= i\frac{g^2(s^2 - c^2)^2}{2\Omega}. \end{aligned}$$

## APPENDIX II

In this appendix, we present the Laplace transform of the two-time correlation function of the cavity field operators appearing in the expression for the incoherent part of the spectrum. We have applied the quantum regression theorem to Eqs. (20) and (21) and calculated the Laplace transform with the initial condition given by the stationary solutions listed in the Appendix I for the case of the cavity frequency tuned on resonance with the central frequency of the dressed-atom system,  $\Delta_c = 0$ .

$$\langle a^\dagger(p), a \rangle_s = \frac{m_4 p^4 + m_3 p^3 + m_2 p^2 + m_1 p + m_0}{2(p + \gamma_1)D(p)}, \quad (39)$$

where

$$D(p) = \alpha\alpha'\gamma_2^2 - [(p + \frac{\kappa}{2})(p + \frac{\kappa}{2} + \gamma_1) - \alpha\alpha']^2, \quad (40)$$

and

$$\begin{aligned}
m_0 &= [2(g_1 \langle R_3 a \rangle_s + \gamma_1 \langle a^\dagger a \rangle_s)(\gamma_1 + \kappa/2) + ((\alpha - \alpha') \langle R_3 a^2 \rangle_s \\
&\quad + (\alpha + \alpha') \langle R_3 a^\dagger a \rangle_s) \gamma_1] [-\kappa(\gamma_1 + \kappa/2)/2 + \alpha \alpha'] \\
&\quad + 2\gamma_1 [\kappa(\gamma_1 + \kappa/2) - 2\alpha \alpha'] (\gamma_1 + \kappa) \langle a \rangle_s \langle a^\dagger \rangle_s \\
&\quad + \gamma_2 (\gamma_1 + \kappa/2) [\gamma_1 ((\alpha + \alpha') \langle a^\dagger a \rangle_s + (\alpha - \alpha') \langle a^2 \rangle_s) \\
&\quad + 2g_1 \alpha \langle R_3 a \rangle_s] + 2\gamma_1 \gamma_2 \alpha \alpha' \langle R_3 a^\dagger a \rangle_s \\
&\quad + 2g_1 [\gamma_1 (\gamma_2 - \alpha)(\gamma_1 + \kappa) + \gamma_2 \kappa (\gamma_1^2 - \kappa^2/4 + \gamma_1 \kappa/2 \\
&\quad + \gamma_2 \alpha + \alpha \alpha') / (2\gamma_1)] \langle a \rangle_s, \\
m_1 &= [2g_1 \langle R_3 a \rangle_s + (4\gamma_1 + \kappa) \langle a^\dagger a \rangle_s + (\alpha - \alpha') \langle R_3 a^2 \rangle_s \\
&\quad + (\alpha + \alpha') \langle R_3 a^\dagger a \rangle_s] [-\kappa(\gamma_1 + \kappa/2)/2 + \alpha \alpha'] \\
&\quad - (\gamma_1 + \kappa) [2(g_1 \langle R_3 a \rangle_s + \gamma_1 \langle a^\dagger a \rangle_s)(\gamma_1 + \kappa/2) \\
&\quad + \gamma_1 (\alpha - \alpha') \langle R_3 a^2 \rangle_s + \gamma_1 (\alpha + \alpha') \langle R_3 a^\dagger a \rangle_s] \\
&\quad + 2[\gamma_1 ((\gamma_1 + \kappa)^2 + \kappa(\gamma_1 + \kappa/2) - 2\alpha \alpha') + (\kappa(\gamma_1 + \kappa/2) \\
&\quad - 2\alpha \alpha') (\gamma_1 + \kappa)] \langle a \rangle_s \langle a^\dagger \rangle_s \\
&\quad + [(2\gamma_1 + \kappa/2)((\alpha + \alpha') \langle a^\dagger a \rangle_s + (\alpha - \alpha') \langle a^2 \rangle_s) \\
&\quad + 2g_1 \alpha \langle R_3 a \rangle_s + 2\alpha \alpha' \langle R_3 a^\dagger a \rangle_s] \gamma_2 \\
&\quad + 2g_1 [(\gamma_2 - \alpha)(2\gamma_1 + \kappa) + \gamma_2 \kappa/2] \langle a \rangle_s, \\
m_2 &= -[(\alpha - \alpha') \langle R_3 a^2 \rangle_s + (\alpha + \alpha') \langle R_3 a^\dagger a \rangle_s] (\kappa + 2\gamma_1) \\
&\quad - g_1 (4\gamma_1 + 3\kappa) \langle R_3 a \rangle_s \\
&\quad + [-\gamma_1 (4\gamma_1 + 3\kappa) - (3\kappa/2 + \gamma_1)(\kappa + 2\gamma_1) \\
&\quad + \gamma_2 (\alpha + \alpha') + 2\alpha \alpha'] \langle a^\dagger a \rangle_s + \gamma_2 (\alpha - \alpha') \langle a^2 \rangle_s \\
&\quad + 2[(\gamma_1 + \kappa)^2 + 2\gamma_1 (\gamma_1 + \kappa) + \kappa(\gamma_1 + \kappa/2) \\
&\quad - 2\alpha \alpha'] \langle a \rangle_s \langle a^\dagger \rangle_s + 2g_1 (\gamma_2 - \alpha) \langle a \rangle_s, \\
m_3 &= -(\alpha - \alpha') \langle R_3 a^2 \rangle_s - (\alpha + \alpha') \langle R_3 a^\dagger a \rangle_s - 2g_1 \langle R_3 a \rangle_s \\
&\quad - 3(2\gamma_1 + \kappa) \langle a^\dagger a \rangle_s + 2(3\gamma_1 + 2\kappa) \langle a \rangle_s \langle a^\dagger \rangle_s, \\
m_4 &= 2(\langle a \rangle_s \langle a^\dagger \rangle_s - \langle a^\dagger a \rangle_s).
\end{aligned}$$